Journal of Low Temperature Physics, Vol. 134, Nos. 1/2, January 2004 (© 2004)

Dynamics of a Highly-Degenerate, Strongly-Interacting Fermi Gas of Atoms

J. E. Thomas, S. L. Hemmer, J. Kinast, A. Turlapov, M. E. Gehm and K. M. O'Hara†

Department of Physics, Duke University, Durham, N.C. 27708-0305, USA
†National Institute of Standards and Technology, Gaithersburg, MD

We use all-optical methods to produce a highly-degenerate, Fermi gas of ^6Li atoms near a Feshbach resonance, where strong interactions are predicted. In this regime, the zero-energy scattering length is larger than the interparticle spacing, and both the mean field energy and the collision rate take on universal forms as a consequence of unitarity and many-body interactions. Our experiments study universal hydrodynamic expansion of the gas and universal mean field interactions. By measuring the cloud radii of the trapped gas, we determine a universal parameter for strongly interacting two-component Fermi systems, the ratio of the mean field energy to the kinetic energy.

PACS numbers: 03.75.Ss, 32.80.Pj.

1. INTRODUCTION

Strongly interacting Fermi systems are predicted to exhibit universal behavior [1]. In trapped atomic gases, such strong forces can be produced in the vicinity of a Feshbach resonance, where a bound molecular state in a closed exit channel is magnetically tuned into coincidence with the total energy of a pair of colliding particles [2]. In this case, the zero energy scattering length a_S, which characterizes the interactions at low temperature, can be tuned through $\pm\infty$. For very large values of $|a_S|$, the important properties of the system (e.g., the effective mean field potential, the collision rate, and the superfluid transition temperature) are predicted to lose their dependence on the magnitude and sign of a_S, and instead become proportional to the Fermi energy with different universal proportionality constants [1].

Theoretical predictions spanning nearly thirty years and several disciplines have been made for the many-body ground state of a strongly-

0022-2291/04/0100-0655/0

interacting two-component Fermi system, characterized by two-body scattering via a short range potential with a very large scattering length [1,3–7].

Recent predictions for neutral atoms include Fermi superfluidity, in which the atomic gas becomes an analog of a superconductor with a very high transition temperature [8–10]. Since the properties of a strongly interacting Fermi gas are predicted to be independent of the zero energy scattering length, desk top measurements on ultracold Fermi gases can be used to test theories in other disciplines, including materials science and condensed matter physics (superconductivity), nuclear physics (nuclear matter), high-energy physics (effective theories of the strong interactions), and astrophysics (compact stellar objects).

In the following, we first review briefly the basic properties of a two-component atomic Fermi gas with strong interactions, and then describe the theory of mean field interactions and hydrodynamic expansion in this regime. The mean field is shown to affect the radii of the trapped gas, which are measured to determine the ratio of the mean field energy to the kinetic energy, an important universal many-body parameter [1].

2. Universal Interactions

In a degenerate Fermi gas, the interparticle spacing L sets the scale of the local Fermi wavevector, $k_F \simeq 1/L$. This is a simple consequence of the Pauli principle which requires no overlap between atomic wave packets with the same spin. The local density n of a gas comprising a 50-50 mixture of two spin components each of density $n/2$ is related to k_F by [11]

$$n(\mathbf{x}) = \frac{k_F^3(\mathbf{x})}{3\pi^2}. \tag{1}$$

When the effective range R of the collision potential is small compared to the interparticle spacing $L \simeq k_F^{-1}$, but the magnitude of the zero-energy scattering length $|a_S|$ is large compared to the interparticle spacing, i.e., $R << L << |a_S|$, the gas is defined to be the intermediate density regime where binary collisions determine the scattering interactions, but the gas is strongly interacting [1]. In the extreme limits, one has approximately, $0 \leq k_F^{-1} \leq \infty$, and the scale of the interaction energy for particles of mass M is determined by the local Fermi energy per particle [12],

$$\epsilon_F(\mathbf{x}) = \frac{\hbar^2 k_F^2}{2M} = \frac{\hbar^2[3\pi^2 n(\mathbf{x})]^{2/3}}{2M}. \tag{2}$$

For a 50-50 mixture of two-spin components, each of density $n/2$, the

local total energy per particle can then be written in the form

$$E(\mathbf{x}) = \frac{3}{5}(1+\beta)\,\epsilon_F(\mathbf{x}) + U_{Trap}(\mathbf{x}), \tag{3}$$

where the first term is local kinetic energy, the second term is the local mean field interaction which is proportional to the local kinetic energy, and

$$U_{Trap} = \frac{M}{2}\left(\omega_x^2 x^2 + \omega_y^2 y^2 + \omega_z^2 z^2\right) \tag{4}$$

is a harmonic trapping potential with oscillation frequencies for atoms moving in the i^{th} direction given by ω_i, $i = x, y, z$. Here β is a universal constant which describes the mean field interaction. Many-body theory predicts that β is always negative when $k_F|a_S| >> 1$ and $|\beta| < 1$ [1,4,6,7].

Many-body theory predicts that β is always negative and $|\beta| < 1$ [1,4,6,7]. In atomic systems with a small scattering length $|a_S| << L$, the mean field energy is proportional to the scattering length, and a negative (positive) scattering length produces an attractive (repulsive) interaction. However, as the zero energy scattering length is tuned toward $+\infty$, an effective attractive interaction arises from the existence of high lying bound molecular states [13]. As the gas expands in thermal equilibrium, existing molecules in these states are converted into free atoms with an associated energy cost.

The equation of state is determined by minimizing the free energy F subject to the constraint that the total number of atoms N is fixed. At zero temperature, $F = E$ where the total energy E is given by

$$E = \int d\mathbf{x}\, n(\mathbf{x}) E(\mathbf{x}) \tag{5}$$

and

$$N = \int d\mathbf{x}\, n(\mathbf{x}). \tag{6}$$

Demanding that the functional derivative of $G(n) = E - \mu N$ with respect to the density n be zero yields the equation of state [14], where μ is the global chemical potential,

$$\mu = (1+\beta)\,\epsilon_F(\mathbf{x}) + U_{Trap}(\mathbf{x}). \tag{7}$$

Defining a scaled Fermi energy ϵ'_F such that $\mu = (1+\beta)\epsilon'_F$ and dividing Eq. 7 by $1+\beta$, it is clear that the equation of state for $\beta \neq 0$ is equivalent to reducing the trapping potential by a factor of $1+\beta$ with ϵ'_F determined by normalization. Hence, for the harmonic oscillator potential of Eq. 4, the effective frequencies for the confining potential are simply scaled according to

$$\omega'_i = \frac{\omega_i}{\sqrt{1+\beta}}. \tag{8}$$

The scaled Fermi energy is simply $\epsilon'_F = \hbar\bar{\omega}'(3N)^{1/3}$ with $\bar{\omega}' = \bar{\omega}/\sqrt{1+\beta}$ and $\bar{\omega} = (\omega_x\omega_y\omega_z)^{1/3}$ the geometric mean of the trap oscillation frequencies.

Using Eq. 2 and Eq. 6, Eq. 7 is easily solved for the density, which takes the form of a Thomas-Fermi distribution [11],

$$n(\mathbf{x}) = n'_F \left(1 - \frac{r'^2}{\sigma'^2}\right)^{3/2} \tag{9}$$

where $r' \leq \sigma'$ and $n'_F = 8N/(\pi^2\sigma'^3)$ is the Fermi (maximum) density. Here, $\sigma' = \sqrt{2\epsilon'_F/(M\bar{\omega}'^2)}$ is the mean Fermi radius. In Eq. 9, $\bar{\omega}^2 r'^2 = \omega_x^2 x^2 + \omega_y^2 y^2 + \omega_z^2 z^2$.

Using

$$\begin{aligned} \frac{r'^2}{\sigma'^2} &= \frac{\omega_x^2 x^2 + \omega_y^2 y^2 + \omega_z^2 z^2}{\bar{\omega}^2\sigma'^2} \\ &= \frac{x^2}{\sigma_x'^2} + \frac{y^2}{\sigma_y'^2} + \frac{z^2}{\sigma_z'^2}, \end{aligned}$$

one obtains the Fermi radii for the interacting gas [14,15],

$$\sigma'_i = \sigma_i\,(1+\beta)^{1/4}, \tag{10}$$

where $\sigma_i = \sqrt{2\epsilon_F/(M\omega_i^2)}$ and $\epsilon_F = \hbar\bar{\omega}(3N)^{1/3}$ is the Fermi energy in the absence of interactions.

Integrating Eq. 9 over y and z, we obtain the one dimensional normalized density distribution for either spin component at zero temperature,

$$\frac{n(x)}{N} = \frac{16}{5\pi\sigma'_x}\left(1 - \frac{x^2}{\sigma_x'^2}\right)^{5/2}. \tag{11}$$

3. Universal Hydrodynamic Expansion

In the strongly interacting regime, the mean field energy is predicted to be proportional to and comparable to the local Fermi energy, as described above. For this case, hydrodynamic expansion is predicted to be independent of the zero energy scattering length and the mean field interaction significantly affects the Fermi radii of the trapped gas. Hence the mean field energy can be determined by measuring the cloud radii. Since the transverse radius of the trapped gas is small, it is convenient to determine it from the radius of the gas after release from the trap.

Strongly interacting Fermi gases exhibit hydrodynamic expansion [16] which can arise from collisionless superfluid hydrodynamics [17] or from collisional hydrodynamics in the unitarity-limited regime where the elastic collision cross is of order $4\pi/k_F^2$ [16,18,19]. In either case the gas expands hydrodynamically after release from the trap, and the radii of the expanding cloud at a given time can be related to that of the trapped gas by a scale transformation.

Whether hydrodynamics arises from collisionless superfluidity or from collisions, the stream velocity $\mathbf{u}$ obeys the equation,

$$M\left(\frac{\partial \mathbf{u}}{\partial t} + \mathbf{u}\cdot\nabla\mathbf{u}\right) = -\nabla\mu(\mathbf{x}), \tag{12}$$

where the local chemical potential $\mu(\mathbf{x})$ is given by Eq. 7.

For irrotational flow, $\nabla \times \mathbf{u} = 0$, and

$$M\frac{\partial \mathbf{u}}{\partial t} = -\nabla\left[(1+\beta)\epsilon_F(n) + \frac{1}{2}M\mathbf{u}^2 + U_{Trap}(\mathbf{x})\right]. \tag{13}$$

The parameter β may differ between the superfluid or normal collisional fluid, i.e., β_S and β_N, respectively.

For both cases, the density-dependent part of the effective potential in Eq. 13 scales with density as a simple power law, since $\epsilon_F(n) \propto n^{2/3}$. Then, for a harmonic trap, the equations of motion admit an exact solution in terms of a scale transformation, where $\tilde{x} = x/b_x(t)$ and $u_x(x,t) = \tilde{x}\,\dot{b}_x(t)$ [17]. The one dimensional density distribution of the expanding gas is then

$$n(x,t) = \frac{1}{b_x(t)}\,n_0\left(\frac{x}{b_x(t)}\right). \tag{14}$$

When the gas is released from the trap, i.e., $U_{Trap} = 0$, the scale factors obey simple equations [17,20] which are independent of β,

$$\ddot{b}_i(t) = \frac{\omega_i^2}{(b_x b_y b_z)^{2/3} b_i}, \tag{15}$$

where $b_i(0) = 1$ and $\dot{b}_i(0) = 0$, for $i = x, y, z$.

The Fermi radii at a time t after the cloud is released from the trap can be determined from the measured one dimensional transverse density profiles $n(x,t)$. These density profiles are obtained by integrating the measured column density $\tilde{n}(x,z,t)$ over z. The total number of atoms $N/2$ in each spin component is obtained by integrating $n(x,t)$ over x.

According to Eq. 14 for hydrodynamic scaling, the density profiles maintain the shape of the initial distribution. One expects that the initial density distribution is a finite temperature Thomas-Fermi distribution.

Then, at a time t after release from the trap, the density of the gas is given by $n(x, \sigma'_x(t), T/T_F)$, where $\sigma'_x(t) = \sigma'_x(0)\, b_x(t)$. The fits yield $\sigma'_x(t)$ which determines then determines the initial Fermi radii in the trap $\sigma'_x(0) = \sigma'_x(t)/b_x(t)$, where $b_x(t)$ is determined from Eq. 15. Eq. 10 then determines β.

4. Experiment

A highly degenerate, two-component Fermi gas is produced by forced evaporation near a Feshbach resonance [21] in our ultrastable CO_2 laser trap. After evaporative cooling, the trap is adiabatically recompressed to full depth and the gas is released from the trap and imaged at various times in the 910 G field to observe the anisotropy. The CO_2 laser power is extinguished in less than 1 μs with a rejection ratio of 2×10^{-5} of the maximum value. A CCD camera images the gas with a magnification of 4.9 from a direction perpendicular to the axial (z) axis of the trap and parallel to the direction (y) of the applied magnetic field.

The gas is rapidly cooled into the highly degenerate regime by subjecting the gas to a 910 G field while lowering the trap laser intensity over 3.5 sec [16]. By inducing evaporative cooling at this field, we avoid the heating and loss which occur at lower fields near 650 G [21]. Further, the collision cross section is very large at 910 G, which is near the predicted Feshbach resonance at 860 G [21]. At this field, we estimate that the gas can be cooled to degeneracy in a fraction of a second. After evaporative cooling, the trap is adiabatically recompressed to full depth and the gas is released from the trap and imaged at various times in the 910 G field to observe the anisotropy. The CO_2 laser power is extinguished in less than 1 μs with a rejection ratio of 2×10^{-5} of the maximum value.

A CCD camera images the gas from direction perpendicular to the axial (z) axis of the trap and parallel to the direction (y) of the applied magnetic field. Resonant absorption imaging on a cycling transition is performed at a fixed high magnetic field by using a weak σ_--polarized (with respect to the y-axis) probe laser pulse of 20 μs duration. The magnification is found to be 4.9 ± 0.15 by moving the axial position of the trap with a micrometer. The spatial resolution is estimated to be $\simeq 4\,\mu$m by quadratically combining the effective pixel size, 13.0 μm/4.9, with the aperture limited spatial resolution of $\simeq 3\,\mu$m.

The trap parameters are obtained using parametric excitation. We find that the trap oscillation frequencies are $\omega_z = 2\pi \times (230 \pm 20)$ Hz for the axial (z) direction and $\omega_\perp = 2\pi \times (6625 \pm 50)$ Hz for the transverse directions.

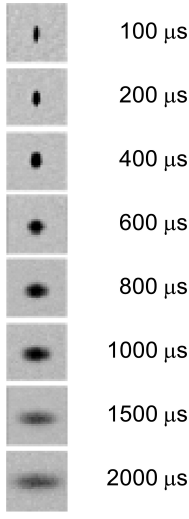

Fig. 1. Anisotropic expansion of a strongly interacting Fermi gas after release from an optical trap. The expansion time varies from 100 μs to 2 ms.

We determine the number of atoms in each state by numerically integrating the column density. For a typical number, $N/2 \simeq 8.0 \times 10^4$ atoms per state, the corresponding Fermi density for the experiments is calculated from Eq. 9 to be $n_F \simeq 4.8 \times 10^{13}/\mathrm{cm}^3$ per state, assuming $\beta = 0$.

The cloud widths $\sigma_x(t)$ and $\sigma_z(t)$ are determined from the measured column density $\tilde{n}(x, z)$ by integrating over z and x respectively and fitting zero temperature Thomas-Fermi distributions, Eq. 11, for each direction.

In Fig. 2, we show the extrapolated initial transverse dimension $\sigma_x(0)$ which is obtained both from the measured $\sigma_x(t)$, i.e, $\sigma_x(0) = \sigma_x(t)/b_x(t)$ and from the measured $\sigma_z(t)$, i.e., $\sigma_x(0) = \lambda\sigma_z(t)/b_z(t)$. Ideal hydrodynamic scaling would produce identical horizontal lines with the same value of $\sigma_x(0)$. In the region where both the axial and transverse plots are nearly horizontal, we obtain $\sigma_x(0) = 3.58 \pm 0.02\,\mu$m. This is in excellent agreement with the value of $\sigma_x(0) = 3.6 \pm 0.1\,\mu$m obtained for the transverse zero-temperature Fermi radius based on the measured atom number and trap frequencies for $\beta = 0$.

Including the temperature correction by using a finite temperature Thomas-Fermi distribution for the fits, we find that the zero temperature radii are smaller by approximately 7%. Eq. 10 then yields a nonzero value of $\beta = -0.26 \pm 0.07$ at 910 G [15]. This value is comparable to the result $\beta = -0.3$ obtained in ^{6}Li at a higher temperature by Bourdel et al. [22], who

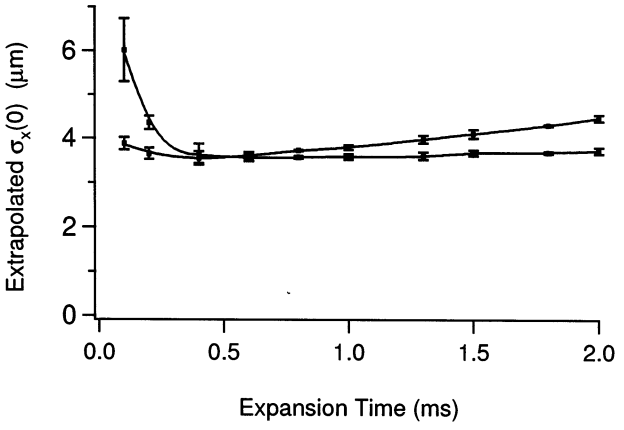

Fig. 2. Extrapolated initial width $\sigma_x(0)$ obtained by scaling the measured transverse and axial dimensions: The nearly horizontal line beyond 0.1 ms shows the results for the transverse direction ($\sigma_x(0) = \sigma_x(t)/b_x(t)$). The axial data ($\sigma_x(0) = \lambda\sigma_z(t)/b_z(t)$) exhibit more deviation from perfect hydrodynamic scaling at long times than the transverse data. The solid curves are added to guide the eye. For ideal hydrodynamic scaling, both should be overlapping horizontal lines.

also showed that β is nearly constant near the Feshbach resonance, suggesting universal behavior. Radio-frequency measurements of mean field shifts in ^{6}Li mixtures also indicate universal behavior [23], while similar measurements in ^{40}K do not [24].

The measured value of β is compared with predictions in Table 1. For our experiments at 910 G, $a_S \simeq -10^4\, a_0$ [21]. Using Eq. 1 and the estimated density yields $k_F a_S = -7.4$. The measured value and the predictions agree in sign but differ by a factor of 2.

5. Conclusions

Fig. 1 shows that the expansion data are reasonably well fit by a scale transformation which can arise from either collisional or superfluid hydrodynamics. Since the density gradient, and hence the force, is much larger in the transverse direction than the axial, one expects that nearly all of the available energy is expended by expansion in the transverse direction. The

Table 1. Predicted values of β.

Prediction	$k_F a_S$	β
Randeria [5]	∞	< -0.410
Baker [4]	∞	-0.674
Baker [4]	∞	-0.432
Steele [6]	∞	-0.674
Steele [6]	-7.4	-0.460
Heiselberg [1]	∞	-0.674
Heiselberg [1]	∞	-0.330
Heiselberg [1]	-7.4	-0.540
Carlson [7]	∞	-0.560

remaining energy in the axial direction is then expected to be very small, producing a slower than ballistic scaling for the axial widths. We find that the transverse data closely matches the hydrodynamic scaling with no free parameters, except at the shortest times, where the transverse radius of the cloud is too small to resolve and diffraction of the light from the cloud produces spurious results for the widths. The axial data fit the expected hydrodynamic scaling to $\simeq 1$ ms. Beyond this time, the axial widths grow faster than expected, suggesting residual thermal energy in the axial direction [25].

One expects that investigation of Fermi gas hydrodynamics in the trap as a function of magnetic field and temperature will enable observation of both collisionless normal and superfluid components at sufficiently low temperature. In addition, precise measurements of the temperature, magnetic field, and time dependence of β will shed new light on universal mean field interactions in strongly interacting Fermi systems.

ACKNOWLEDGMENTS

This research is supported by the Physics Divisions of the Army Research Office and the the National Science Foundation, the Fundamental Physics in Microgravity Research program of the National Aeronautics and Space Administration, and the Chemical Sciences, Geosciences and Biosciences Division of the Office of Basic Energy Sciences, Office of Science, U. S. Department of Energy.

REFERENCES

1. H. Heiselberg, *Phys. Rev. A* **63**, 043606 (2001).
2. See E. Tiesinga, B. J. Verhaar, and H. T. C. Stoof, *Phys. Rev. A* **47**, 4114 (1993) and references therein.
3. G. A. Baker, Jr., *Rev. Mod. Phys.*, **43**, 479 (1971).
4. G. A. Baker, Jr., *Phys. Rev. C* **60**, 054311 (1999).
5. M. Randeria, *et al.*, *Phys. Rev. B* **55**, 15153 (1997).
6. J. V. Steele, e-print nucl-th/0010066 (2000).
7. J. Carlson, *et al.*, *Phys. Rev. Lett.* **91**, 050401 (2003).
8. M. Holland, *et al.*, *Phys. Rev. Lett.* **87**, 120406 (2001).
9. E. Timmermans, *et al.*, *Phys. Lett. A* **285**, 228 (2001).
10. Y. Ohashi and A. Griffin, *Phys. Rev. Lett.* **89**, 130402 (2002).
11. D. A. Butts and D. S. Rokhsar, *Phys. Rev. A* **55**, 4346 (1997).
12. This argument was suggested to us by R. Furnstahl, Ohio State University, private communication.
13. J. Ho and E. Mueller, e-print cond-mat/0306187 (2003).
14. This method of deriving the equation of state was provided by S. Stringari, private communication.
15. M. E. Gehm, *et al.*, *Phys. Rev. A* **68**, 011401(R) (2003).
16. K. M. O'Hara, *et al.*, *Science* **298**, 2179 (2002).
17. C. Menotti, *et al.*, *Phys. Rev. Lett.* **89**, 250402 (2002).
18. L. Pitaevski and S. Stringari, *Science* **298**, 2144 (2002).
19. M. E. Gehm, *et al.*, *Phys. Rev. A* **68**, 011603(R) (2003).
20. Y. Kagan, *et al.*, *Phys. Rev. A* **55**, 18 (1997).
21. K. M. O'Hara, *et al.*, *Phys. Rev. A* **66**, 041401(R) (2002).
22. T. Bourdel, *et al.*, e-print cond-mat/0303079 (2003).
23. S. Gupta, *et al. Science* **300**, 1723(2003).
24. C. A. Regal and D. S. Jin, *Phys. Rev. Lett.* **90**, 230404 (2003).
25. This idea was suggested to us by J. Walraven, private communication.